PHILOSOPHICAL TRANSACTIONS OF THE ROYAL SOCIETY A MATHEMATICAL, PHYSICAL & ENGINEERING SCIENCES

Interaction of steep waves with offshore structures

Eatock Taylor and G. X. Wu

Phil. Trans. R. Soc. Lond. A 1997 **355**, 593-605
doi: 10.1098/rsta.1997.0027

Interaction of steep waves with offshore structures

By R. Eatock Taylor[1] and G. X. Wu[2]

[1]*Department of Engineering Science, University of Oxford, Parks Road, Oxford OX1 3PJ, UK*

[2]*Department of Mechanical Engineering, University College London, London WC1E 7JE, UK*

Offshore structures having large diameter columns at the waterline cause a significant disturbance to the ambient wave field, and large run-up around the columns. The paper discusses prediction of this effect in regular sinusoidal waves and in focused wave groups characteristic of extreme storm waves. Results are obtained from linear and second-order nonlinear analytical solutions for vertical circular cylinders. For very large waves, however, a fully nonlinear analysis is needed, which must be based on numerical discretization in both temporal and spatial dimensions. A finite-element procedure for predicting the interaction of steep waves with offshore structures is briefly introduced.

1. Introduction

Motivated to a large extent by developments in the offshore industry, there has been, over the last 25 years, a considerable corpus of research into the diffraction of water waves. Analytical solutions have been obtained for bodies of simple geometry in sinusoidal waves, and numerical methods have been developed to solve the potential flow problem for structures of arbitrary geometry at or near the free surface. It is assumed in such work that the characteristic dimensions of the structure are sufficiently large that separation effects due to viscosity can be ignored. Where this is not the case it has been traditional to use the semi-empirical Morison equation in offshore design, although recent advances in obtaining numerical solutions of the Navier–Stokes equations are beginning to have an influence.

The emphasis during this period has largely been on the estimation of hydrodynamic forces. These provide the necessary loading conditions for an assessment of ultimate structural strength and fatigue life, and for estimating the motions of floating structures. It is only much more recently that interest has been taken in the disturbance to the free surface resulting from wave diffraction, and in the considerable magnification effects which can affect wave elevations locally. This seems to have arisen for a combination of reasons. Historically the industry has been dominated by the use of fixed platforms, mostly constructed of tubular members which do not significantly disturb the incident wave field. The design ‘air-gap’ between the underside of the deck and the highest predicted undisturbed storm wave at the location of the structure, in the highest astronomical tide, could be minimal, reflecting mainly uncertainties in prediction of maximum undisturbed wave height. In the exceptional

Phil. Trans. R. Soc. Lond. A (1997) **355**, 593–605
Printed in Great Britain

cases of the large diameter columns of gravity platforms, it was easy to design for an increased air gap: the cost of raising the height of the columns was not thought sufficient to call for great accuracy in the prediction of the disturbed wave elevation and simple approaches were deemed acceptable. Recent experiments, however, have demonstrated higher than expected local elevations, leading to expensive changes in design or operational procedure for both fixed and floating platforms. This is particularly critical for weight sensitive structures such as certain tension leg platforms (TLPs). To permit economic exploitation for moderate accumulations of hydrocarbons in deep-water hostile areas, such as West of Shetlands, new types of TLP are being developed. These are carefully optimized for pay-load capacity, and there is a trade-off between pay-load and deck height: increasing the latter without reducing the former requires a larger buoyant hull, hence larger vertical wave loads and greater difficulty in maintaining minimum tether tension. The significance of local wave disturbances, and run-up around columns, is not however restricted to TLPs and fixed structures. Reports of damage beneath the lowest decks of semisubmersible platforms provide further incentive for investigating this problem.

This paper provides a brief review of approaches for predicting localized wave disturbance effects due to diffraction. First we illustrate the application of standard *linear* diffraction theory. The disturbance by a circular cylinder in sinusoidal waves is compared with the behaviour in a focused wave group (characterizing the largest wave in a random seaway). Linear theory, however, is a poor model for conditions in extreme waves. The importance of nonlinear interactions in a focused wave group has very recently been highlighted by the experimental work of Baldock *et al.* (1996). This concerned incident waves alone, but it is clear that such interactions will also affect waves scattered by structures. An understanding of such effects can be sought by extending linear theory to *second order*, using the expansion procedure first suggested in the context of nonlinear water waves by Stokes (1847). Much research has concentrated on the analysis of second-order wave diffraction forces. In our own recent work (Wu 1991; Chau & Eatock Taylor 1992; Eatock Taylor & Chau 1992; Huang & Eatock Taylor 1996) we have attempted to develop semianalytical and fully numerical methods which yield the second-order wave elevation at any point, and more generally the complete flow field. We review some features of this work below, and illustrate its application to analysis of the second-order disturbance of an incident wave group.

Ultimately, of course, understanding of the interaction of extreme wave groups with offshore structures requires a *fully nonlinear* analysis. Methods are being developed in the context of assessing 'ringing' loads, characterized by large high-frequency transient components of force when a steep wave encounters a structure. Insight into the occurrence of such forces is being gained from approximate analyses for cylinders, based on various assumptions of slenderness (Rainey 1995; Faltinsen *et al.* 1995). Such approximations, however, are inevitably unable to provide reliable quantitative indications of wave disturbance effects. The only viable approach for predicting the disturbance by large bodies, even for the simple geometry of a vertical cylinder, would appear to involve full numerical discretization. Ferrant (1995) has used a boundary-element method. Volume-based discretization procedures for solving the fully nonlinear wave diffraction problem are also being developed. Mehlum (1993) uses a spline representation; and a finite-element discretization is being developed by Cai *et al.* (1996). Wu & Eatock Taylor (1994, 1995), Greaves *et al.* (1995) and Wu *et al.* (1996) have obtained results from both two- and three-dimensional finite-element

formulations for transient nonlinear wave diffraction problems, and the present paper concludes by briefly summarizing this approach.

2. Linear analysis of waves interacting with circular cylinders

(*a*) *Cylinders in sinusoidal waves*

The linear diffraction problem for a single vertical cylinder in deep-water sinusoidal waves was first solved by Havelock (1940). It is summarized here, as it forms the basis for what follows. The fluid is incompressible and irrotational, and the problem is posed in terms of a velocity potential $\Phi(x, y, z, t)$. The origin of the Cartesian coordinate system is located at the intersection of the mean free surface with the axis of the cylinder, and the z-axis is directed positive upwards. It is also convenient to use polar coordinates (r, θ, z), where $x = r\cos\theta$, $y = r\sin\theta$.

We first consider the linear diffraction problem in which the incident waves are sinusoidal having frequency ω, and amplitude A, propagating in the direction of positive x. The water has depth d. We take

$$\Phi(x, y, z, t) = \mathrm{Re}\{A\phi(x, y, z)\mathrm{e}^{-\mathrm{i}\omega t}\}, \tag{2.1}$$

and decompose the complex potential ϕ into incident (I) and diffracted (D) components, respectively. The incident potential is written

$$\phi_{\mathrm{I}} = -\frac{\mathrm{i}g}{\omega}\frac{\cosh(k(z+d))}{\cosh(kd)}\mathrm{e}^{\mathrm{i}kx} = -\frac{\mathrm{i}g}{\omega}\frac{\cosh(k(z+d))}{\cosh(kd)}\sum_{n=0}^{\infty}\epsilon_n \mathrm{i}^n J_n(kr)\cos(n\theta), \tag{2.2}$$

where $\epsilon_0 = 1, \epsilon_n = 2$ for $n > 0$. The wave number k is given by $k\tanh(kd) = \omega^2/g$. ϕ satisfies the linear free surface condition for no flow through the surface of the cylinder $(r = a)$, where the radius of the cylinder is a. ϕ_{D} also satisfies the radiation condition for outgoing waves. The solution to this boundary value problem, as obtained by Havelock (1940), is

$$\phi(r, \theta, z) = -\frac{\mathrm{i}g}{\omega}\frac{\cosh(k(z+d))}{\cosh(kd)}\left[\mathrm{e}^{\mathrm{i}kr\cos\theta} - \sum_{n=0}^{\infty}\epsilon_n \mathrm{i}^n \frac{J_n'(ka)H_n^{(1)}(kr)}{H_n^{(1)'}(ka)}\cos n\theta\right]. \tag{2.3}$$

From this we obtain the linear wave force on the cylinder, and the run-up, which we define as the modulus of the non-dimensional free surface elevation around the waterline. The behaviour of the linear force on the single cylinder is extremely well known, and we do not consider this here. The run-up is

$$\eta(a, \theta) = \left|\frac{\mathrm{i}\omega}{g}\phi\right| = \left|\mathrm{e}^{\mathrm{i}ka\cos\theta} - \sum_{n=0}^{\infty}\epsilon_n \mathrm{i}^n \frac{J_n'(ka)H_n^{(1)}(ka)}{H_n^{(1)'}(ka)}\cos n\theta\right|. \tag{2.4}$$

This quantity is shown as a surface in figure 1, plotted against θ and ka. For small values of ka (long waves), the effect of diffraction is negligible, and the run-up is everywhere close to one corresponding to the incident wave. For high values of ka (short waves), the behaviour upwave approximates to pure reflection of a plane wave by a wall, and the run-up is close to two; but behind the cylinder, in the shadow region, the run-up is of course close to zero.

These results are of considerable practical relevance, though they have in the past often been disregarded. In the range of typical geometries, the values of ka corresponding to severe storm waves can be such that the run-up is considerably

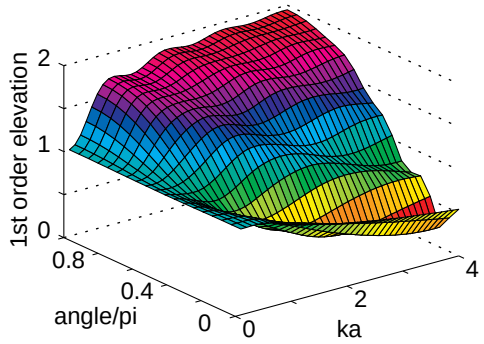

Figure 1. Wave number dependence of run-up at a vertical cylinder.

greater than one. Consider, for example, a column of a large tension leg platform having a radius of 15 m: in a sinusoidal wave of 10 s period in deep water the incident wave amplitude would be increased locally by 56% as a result of diffraction by the column considered in isolation (i.e. ignoring the additional amplification that can be caused by interaction effects between the columns, Eatock Taylor & Sincock 1989). It might be assumed that by simply increasing the under deck air-gap the designer could avoid the implications of such local increases in wave elevation. This overlooks the fact that these platforms can be highly weight sensitive, and increasing the height of the deck by adding structure may not be a viable option.

(*b*) *Cylinders in a wave group*

The preceding discussion has focused attention on run-up in regular sinusoidal waves. A more realistic design condition, however, is the large wave group in a random seaway. We consider here the critical case of long-crested random waves. It has been shown by Boccotti (1983) and Tromans *et al.* (1991) that under appropriate conditions of ergodicity and linear random wave theory, the highest wave tends to a profile proportional to the time history which is given by the autocorrelation function for the wave elevation process. We now seek to establish the characteristics of the run-up in such a case.

By way of illustration, we examine the conditions in a storm defined by the International Towing Tank Conference (ITTC) wave spectrum (see for example Price & Bishop 1974). The one-sided ITTC frequency spectrum is written (in units of metres and seconds) as

$$G(\omega) = \frac{0.0081g^2}{\omega^5} \exp\left(\frac{-3.11}{H_s^2\omega^4}\right), \tag{2.5}$$

where H_s is the 'significant' wave height. We shall use the dimensionless form

$$\Gamma(\sigma) = \frac{0.0081}{\sigma^5} \exp\left(\frac{-3.11}{g^2h^2\sigma^4}\right), \tag{2.6}$$

where

$$\sigma = \omega\sqrt{a/g} = \sqrt{ka}; \quad h = H_s/a. \tag{2.7}$$

(We are assuming deep-water waves). The corresponding dimensionless time autocorrelation function is

$$\rho(\tau) = \int_{-\infty}^{\infty} \Gamma(\sigma)\mathrm{e}^{-\mathrm{i}\sigma\tau}\,\mathrm{d}\sigma, \tag{2.8}$$

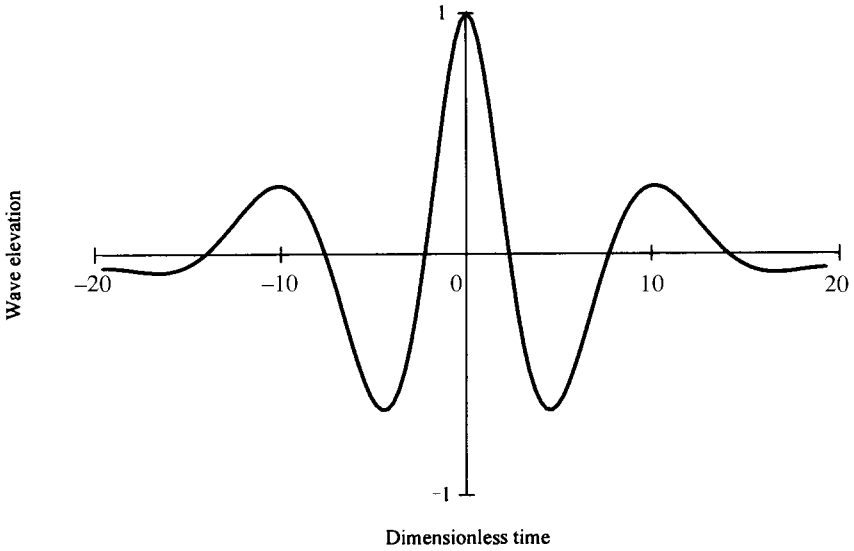

Figure 2. Time history of the largest wave group in an ITTC seaway ($h = 0.5$)

.

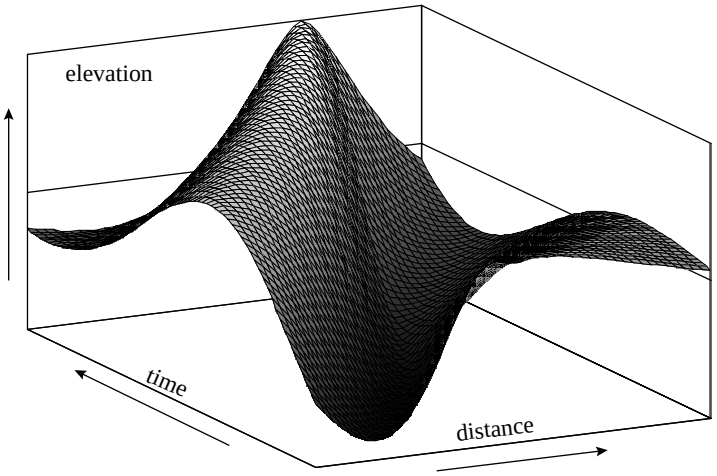

Figure 3. Spatial evolution of the wave group.

where $\tau = t\sqrt{g/a}$. The time history of the extreme wave group is then proportional to $\rho(\tau)$ in the region around $\tau = 0$. Figure 2 shows such a wave group (for the case $h = 0.5$), scaled to have a unit value at the crest. The spatial profile may be obtained in a similar manner from the wave number spectrum. The evolution of the group may then be shown as a surface, plotted against the axes of space and time. This is given in figure 3, where time has been non-dimensionalized as above, and the spatial axis is x/a.

We now examine the run-up at the cylinder resulting from diffraction of this wave group. We consider the case when the group is focused such that the incident wave peaks at the location of the upper face of the cylinder. Figure 4 shows cross-sections of the wave through the plane $y = 0$. Figures 4*a–c* correspond to the three storms defined by $h = 0.25$, $h = 0.5$ and $h = 1.0$, respectively. In each case the incident wave

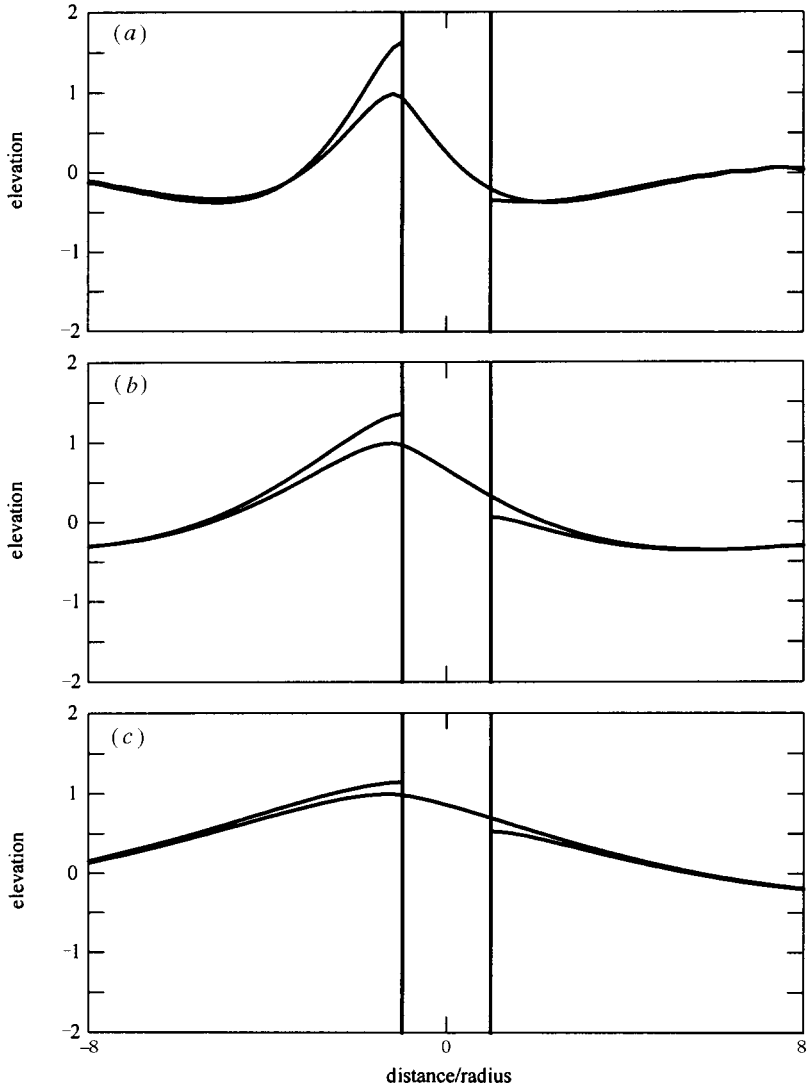

Figure 4. Total scattered wave profiles in 3 ITTC wave groups: (*a*) $h = 0.25$; (*b*) $h = 0.5$; (*c*) $h = 1.0$.

group is shown, together with the total scattered wave (incident plus diffracted), at the time when the total elevation is a maximum at the upwave face (the left of the two vertical lines denoting the cylinder). It is found that in the lowest of the three seastates (having components at the highest frequencies), the incident wave elevation is increased by 61% at the upwave face.

The analysis of Boccotti (1983) suggests that one can define a linear sinusoidal wave which locally is close to the linear focused wave group, by choosing the wave period $T_s \approx 1.2T_z$ (where T_z is the mean zero up-crossing period of the random sea state giving rise to the group). The corresponding dimensionless frequency is $\sigma_s \approx 0.47/\sqrt{h}$ (based on the definition in equation (2.7)), which is somewhat higher than the frequency of the peak of the wave spectrum, $\sigma_p = 0.40/\sqrt{h}$. Figure 5 compares the profiles of the wave group and a closely equivalent sinusoidal wave ($\sigma_p = 0.45/\sqrt{h}$),

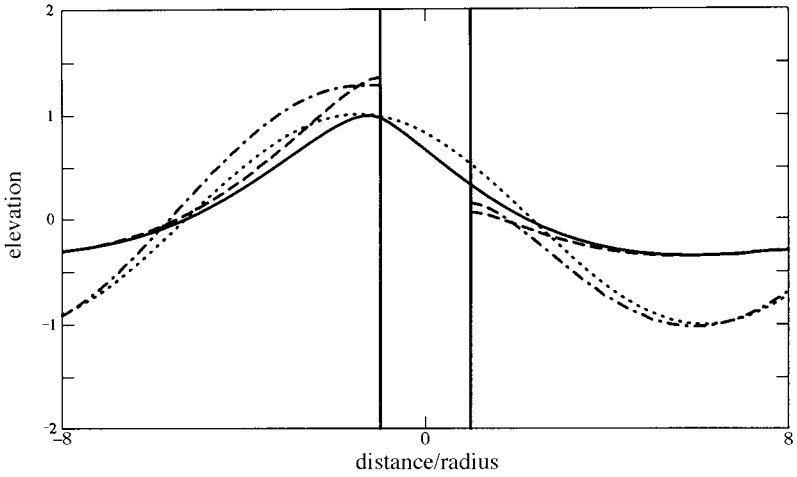

Figure 5. Wave profiles in a sinusoidal wave and in an ITTC wave group: ——, ITTC incident; – – –, ITTC scattered; · · · · · ·, sine incident; — · — · —, sine scattered.

together with the associated total scattered waves, for the case when $h = 0.5$. The results are plotted at the time when the wave group gives maximum run-up (which is just before the crest reaches the upwave face). It is seen that the sinusoidal wave leads to similar behaviour, and in spite of the wave group having its maximum energy at a lower frequency, it still leads to a significant increase in local elevation due to the effect of diffraction. This effect can also be reproduced in an appropriately chosen bichromatic wave group, as discussed below in the context of nonlinear analysis.

The single cylinder linear diffraction analysis may readily be extended to the case of multiple vertical cylinders. Linton & Evans (1990) described an effective procedure, based on use of the Bessel addition theorem. Because of the interactions between the cylinders, large local amplifications can occur both at the cylinders and on any plane of symmetry parallel to the wave direction. This was demonstrated numerically in the results of Eatock Taylor & Sincock (1989). Recently, Maniar & Newman (1996) and D. V. Evans (1996, personal communication) have shown that, for certain spacings of the cylinders, trapped waves can exist. The flow field in a regular wave whose frequency corresponds to a trapped mode can be expected to be characterized by extremely high local wave elevations.

All this, however, is based on simple linear theory, which still forms the basis for design calculations of run-up around the large diameter columns of offshore platforms. Nonlinear effects can be expected to limit the very high local elevations predicted in the case of trapped modes excited by multiple cylinders in regular waves. On the other hand, nonlinear interactions between the various components can significantly increase the peak elevation in a wave group (see, for example, Longuet Higgins & Stewart 1960; Baldock *et al.* 1996).

It is convenient to investigate such effects by extending the linear analysis to second order, based on the expansion procedure of Stokes (1847). This requires solution of the second-order diffraction problem.

3. Second-order analysis

The analysis of second-order diffraction by a single vertical circular cylinder has received considerable attention in recent years, largely in the context of obtaining

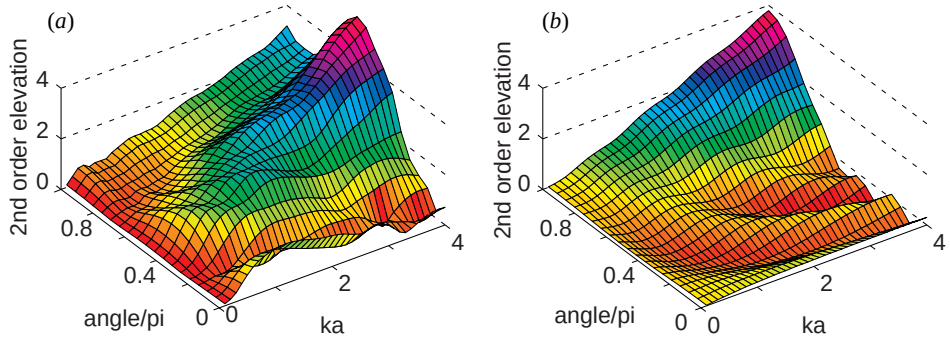

Figure 6. Wavenumber dependence of second-order run-up at a vertical cylinder: (*a*) double frequency component; (*b*) mean component.

expressions for second-order forces. Thus it has been shown, for example by Lighthill (1979) and Molin (1979), that provided only forces are required, a technique can be applied that avoids the need to solve directly for the second-order potential in the Stokes expansions. Eatock Taylor & Hung (1987) used this technique to obtain a semianalytical formulation for the second-order force on a single cylinder in regular waves, and Kim & Yue (1990) gave results for a single cylinder in bichromatic waves. Moubayed & Williams (1995) developed the corresponding analysis and results for second-order forces on multiple vertical cylinders, based on the interaction theory of Linton & Evans (1990). A detailed further investigation of the second-order force on the single cylinder in regular waves has recently been completed by Newman (1996). In particular, he has obtained consistent asymptotic expansions for the limits of long and short wave lengths. This has led to the important conclusion that the slender body approximation becomes inaccurate at surprisingly small values of dimensionless wave number (i.e. the accuracy deteriorates rapidly as ka exceeds 0.1).

In order to compute the free surface elevation and wave kinematics, it is necessary to solve for the second-order potential directly. Chau & Eatock Taylor (1992) gave the analysis for a single vertical cylinder in regular waves, and this was extended by Huang & Eatock Taylor (1996*a*, *b*) to truncated cylinders and bichromatic waves. Extending equation (2.1), we can express the potential in the form of the Stokes expansion

$$\Phi(x,y,z,t) = \mathrm{Re}\left\{\sum_{j=1}^{2} A_j \phi_j^{(1)}(x,y,z)\mathrm{e}^{-\mathrm{i}\omega_j t} + \sum_{j=1}^{2}\sum_{k=1}^{2}[A_j A_k^* \phi_{jk}^-(x,y,z)\mathrm{e}^{-\mathrm{i}\omega_{jk}^- t} + A_j A_k \phi_{jk}^+(x,y,z)\mathrm{e}^{-\mathrm{i}\omega_{jk}^+ t}]\right\}, \quad (3.1)$$

where A_j is the complex amplitude of the jth component and $\omega_{jk}^{\pm} = (\omega_j \pm \omega_k)$.

Any force or kinematic quantity may then be expressed in the form

$$X(t) = \mathrm{Re}\left\{\sum_{j=1}^{2} A_j H_j^{(1)}(\omega_j)\mathrm{e}^{-\mathrm{i}\omega_j t} + \sum_{j=1}^{2}\sum_{k=1}^{2} A_j A_k^* H_{jk}^-(\omega_j,-\omega_k)\mathrm{e}^{-\mathrm{i}\omega_{jk}^- t} + \sum_{j=1}^{2}\sum_{k=1}^{2} A_j A_k H_{jk}^+(\omega_j,\omega_k)\mathrm{e}^{-\mathrm{i}\omega_{jk}^+ t}\right\}. \quad (3.2)$$

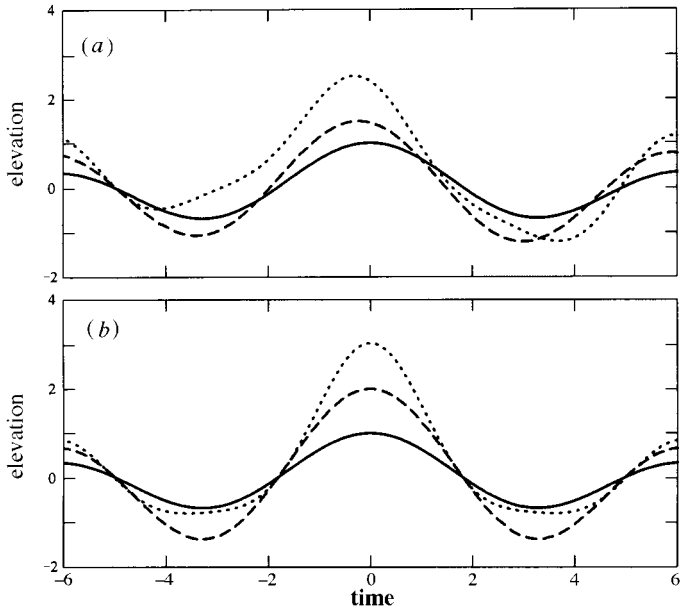

Figure 7. Time histories of a bichromatic wave group and of first and second-order run-up: ——, first-order incident wave; – – –, first-order scattered wave; ·····, first- and second-order scattered wave: (*a*) at a vertical cylinder; (*b*) at a wall.

$H^{(1)}$ and $H^{\pm}$ are the linear and quadratic transfer functions, respectively, the latter providing for both sum and difference frequency components. The quadratic transfer function (QTF) for the second-order sum frequency elevation can be written

$$H^{+}_{jk} = \left\{ -\frac{1}{4g}\nabla\phi^{(1)}_{j}\nabla\phi^{(1)}_{k} + \frac{\omega_j\omega_k}{2g^2}\phi^{(1)}_{j}\frac{\partial\phi^{(1)}_{k}}{\partial z} - \frac{\mathrm{i}\omega^{+}_{jk}}{g}\phi^{+}_{jk} \right\}\Bigg|_{z=0}. \tag{3.3}$$

For the corresponding difference frequency QTF, the superscripts + are replaced by −, and in the products the second term of each pair is replaced by its conjugate.

Calculation of the QTFs involves solving for the important second-order potentials $\phi^{\pm}$. These comprise contributions from 'free' wave components, and 'locked' waves resulting from the inhomogeneous boundary condition satisfied by the second-order potential on the free surface. The solution for the latter component can be expressed in terms of a line integral over $(a < r < \infty)$, which is highly oscillatory and converges very slowly as $r \to \infty$. Details of this analysis are given by Chau & Eatock Taylor (1992) and Huang & Eatock Taylor (1996*a*). The semianalytical solutions for truncated vertical cylinders and groups of cylinders are given in Huang & Eatock Taylor (1996*b*).

As an illustration of the second-order results for run-up, we consider the case of the cylinder of radius a and plot the diagonal terms of the QTFs for $\eta^{\pm}(a,\theta)$ as functions of ka and θ (analogous to the linear run-up plotted in figure 1). Figures 6*a* and 6*b* are for the sum and difference frequency terms, respectively, which in this case correspond to $\omega^{+}_{jk} = 2\omega$ and $\omega^{-}_{jk} = 0$. The calculations have been performed for a cylinder in water of depth 20 times the radius. The double frequency QTF is shown as the non-dimensional modulus $k|H^{+}_{jk}|$, and the mean QTF, being real, is shown as kH^{-}_{jk}. We recalled previously that the high-frequency limit of the linear run-up at the upwave face of the cylinder corresponds to pure reflection, hence a

100% increase on the incident amplitude. The corresponding second-order solution for pure reflection by a plane wall can also be simply obtained. For deep-water waves the QTFs reduce to the form

$$H_{jk}^{+} = -(\omega_j^2 + \omega_k^2 - \omega_j\omega_k)/g = H_{jk}^{-}. \tag{3.4}$$

Hence the high-frequency limits of the diagonal terms of both sum and difference frequency QTFs for wave elevation at the upwave face of the cylinder in deep water both reduce to the wave number of the first-order incident wave. This can be clearly seen in figures 6*a*, *b*.

The wave elevation run-up QTF can now be used to investigate the effect of nonlinear wave–wave interactions when a large wave group encounters the cylinder. Let us illustrate this by considering a linear deep-water bichromatic wave group, encountering a cylinder of radius $a = 10$ m. We choose frequency components defined in dimensionless form by $k_1a = \omega_1^2(a/g) = 0.4$ and $k_2a = \omega_2^2(a/g) = 1.6$; the amplitudes are taken as $A_1/a = 0.2$, $A_2/a = 0.4$; and the components are in phase at $t = 0$ at the upwave face of the cylinder. The time history of the elevation of the undisturbed first-order incident wave group at the upwave face is shown as the solid line in figure 7*a* (divided by $(A_1 + A_2)$). This is similar to the ITTC wave groups shown in figure 4. The dashed line shows the total corresponding linear scattered wave (divided by $(A_1 + A_2)$). Also shown in figure 7*a* (dotted) is the total run-up to second order (divided by $(A_1 + A_2)$): i.e. this includes all first and second-order contributions. For comparison the corresponding results for the plane wall are shown in figure 7*b*. In this time history one notes clearly the sharpening of the crest and flattening of the trough.

These and similar results give an indication of the influence of second-order effects on run-up. In extreme waves, however, it is likely that higher-order nonlinearities may also be important, and there is therefore a need for fully nonlinear analysis of the diffraction problem.

4. Nonlinear simulations

To solve the fully nonlinear problem requires numerical discretization in both space and time. Boundary-element methods have proved popular for solving the linear and second-order diffraction problems in the frequency domain. These lead to fully populated coefficient matrices of Green functions and their derivatives, which are frequency dependent. Typically only the surface of the body needs to be discretized, and results are only required at a relatively small number of frequencies; hence the time to compute the solution of the matrix equations for realistic discretizations is usually now manageable on modern workstations. For the nonlinear problem in the time domain, however, the discretization must be regularly updated as the wave field evolves, and the resulting matrix must be solved at a very large number of time steps. This has led us to conclude that an adaptive mesh finite-element discretization is preferable, in which one can exploit the small bandwidth of the resulting coefficient matrices. Although the total number of unknowns in the three-dimensional finite-element discretization is substantially greater than in the boundary-element representation of the same problem, the time to solve the matrix equations can be much less (Wu & Eatock Taylor 1995). This has been confirmed by Cai *et al.* (1996).

Wu & Eatock Taylor (1994, 1995) and Greaves *et al.* (1995) have developed such

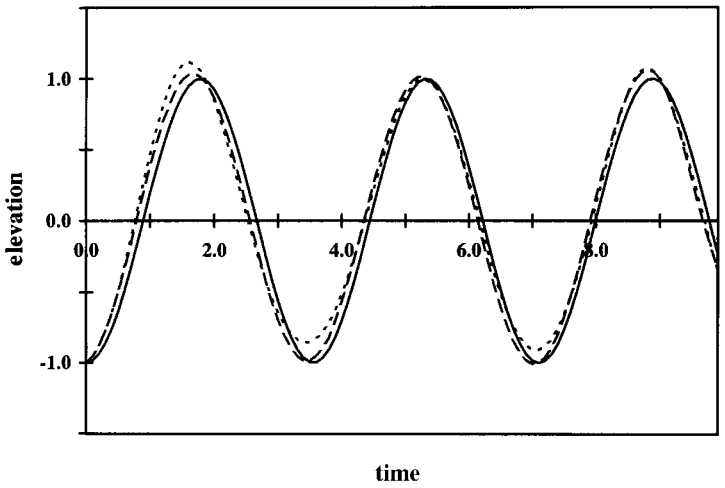

Figure 8. Results from finite-element analysis of wave evolution in a rectangular tank: – – –, $A/d = 0.01$; · · · · · ·, $A/d = 0.05$; ——, analytical.

a formulation for the restricted case of two-dimensional flow in the vertical plane. The extension to three dimensions is given in Wu *et al.* (1996). They show how a domain–decomposition method can be used to divide the flow field into separate domains, in each of which the solution at each time step is first solved independently of neighbouring domains. Continuity between domains is then achieved through a process of iteration. To investigate the propagation of a transient wave past a structure, it is unnecessary to consider the domains downstream of the wave front. This approach can be combined with the idea of energy absorbing layers to effect suitable radiation conditions downstream of the structure (as used for example in the boundary-element approach of Ferrant (1995)).

In the process of validating the adaptive mesh three-dimensional nonlinear simulation, we have considered the response to an initial free surface disturbance in a rectangular tank. Figure 8 shows the time history of free surface elevation at the centre of a tank of length $2d$ and width $0.3d$, where d is the depth of water. The mesh is based on dividing the rectangular volume by 21 transverse $\times$ 7 longitudinal $\times$ 17 horizontal planes, leading to 1920 bricks, each of which is subdivided into six tetrahedral finite elements (i.e. 11520 in total). The initial disturbance is two-dimensional, varying down the length of the tank as a cosine of amplitude A and wave length $2d$, with the crest in the centre at $t = 0$. The figure compares two cases ($A/d = 0.01, 0.05$) with the analytical solution for the corresponding linear standing wave, which has frequency $\sigma = (\pi \tanh \pi)^{0.5}$. (The frequency and time are here non-dimensionalized as in § 2, with d replacing a. The time step was $\Delta\tau = 0.1$.) The results are analogous to those from the two-dimensional cases considered by Wu & Eatock Taylor (1994), but satifying the further (non-trivial) test that the wave remains sensibly two-dimensional in the three-dimensional simulation.

This and related test cases are confirming the viability of the finite-element solution procedure. When the second-order theory reviewed in § 3 ceases to be valid, it is approaches such as these which must be employed to simulate a steep wave group encountering a complex offshore structure. The computational effort will be substantial, but it is only by this means that reliable theoretical predictions can be made for realistic extreme conditions.

This work forms part of the research programme 'Uncertainties in loads on offshore structures' sponsored by EPSRC through MTD Ltd and jointly funded with: Aker Engineering a.s., Amoco (UK) Exploration Company, BP Exploration Operating Co. Ltd, Brown & Root, Exxon Production Research Company, Health and Safety Executive, Shell UK Exploration and Production, Statoil, Texaco Britain Ltd. Dr J. B. Huang and Mr Q. W. Ma are thanked for their assistance in developing the analyses summarized here.

References

Baldock, T. E., Swan, C. & Taylor, P. H. 1996 A laboratory study of nonlinear surface waves on water. *Proc. R. Soc. Lond.* A **354**, 649–676.

Boccotti, P. 1983 Some new results on statistical properties of wind waves. *Appl. Ocean Res.* **5**, 134–140.

Cai, X., Langtangen, H. P., Nielsen, B. F. & Tveito, A. 1996 A finite element method for fully nonlinear water waves. Preprint 1996-3, Department of Informatics, University of Oslo.

Chau, F. P. & Eatock Taylor, R. 1992 Second-order wave diffraction by a vertical cylinder. *J. Fluid Mech.* **240**, 571–599.

Eatock Taylor, R. & Chau, F. P. 1992 Wave diffraction theory—some developments in linear and nonlinear theory. *J. Offshore Mech. Arctic Engng* **114**, 185–194.

Eatock Taylor, R. & Hung, S. M. 1987 Second-order diffraction forces on a vertical cylinder in regular waves. *Appl. Ocean Res.* **9**, 19–30.

Eatock Taylor, R. & Sincock, P. 1989 Wave upwelling effects in TLP and semisubmersible structures. *Ocean Engng* **16**, 281–306.

Faltinsen, O. M., Newman, J. N. & Vinje, T. 1995 Nonlinear wave loads on a slender vertical cylinder. *J. Fluid Mech.* **289**, 179–198.

Ferrant, P. 1995 Nonlinear wave loads and run-up upon a surface-piercing cylinder. In *Proc. 10th Int. Workshop on Water Waves and Floating Bodies, Oxford, 2–5 April 1995* (ed. R. Eatock Taylor), pp. 57–60.

Greaves, D. M., Borthwick, A. G. L. B., Eatock Taylor, R. & Wu, G. X. 1995 Analysis of wave-body interactions using adaptive finite element meshes. In *Proc. 10th Int. Workshop on Water Waves and Floating Bodies, Oxford, 2–5 April 1995* (ed. R. Eatock Taylor), pp. 83–87.

Havelock, T. H. 1940 The pressure of water waves on a fixed obstacle. *Proc. R. Soc. Lond.* A **175**, 409–421.

Huang, J. B. & Eatock Taylor, R. 1996*a* Semianalytical solution for second-order wave diffraction by a truncated circular cylinder in monochromatic waves. *J. Fluid Mech.* **319**, 171–196.

Huang, J. B. & Eatock Taylor, R. 1996*b* Application of second-order diffraction analysis to TLP design. Final Report on Project A4, Managed Programme on Uncertainties in Loads on Offshore Structures, Department of Engineering Science, University of Oxford.

Kim, M. H. & Yue, D. K. P. 1990 The complete second-order diffraction solution for an axisymmetric body. 2. Bichromatic incident waves and body motions. *J. Fluid Mech.* **211**, 557–593.

Lighthill, M. J. 1979 Waves and hydrodynamic loading. In *Proc. 2nd Int. Conf. Behaviour Offshore Structures, BOSS79 London*, pp. 1–40.

Linton, C. M. & Evans, D. V. 1990 The interaction of waves with arrays of vertical circular cylinders. *J. Fluid Mech.* **215**, 549–569.

Longuet-Higgins, M. S. & Stewart, R. W. 1960 Changes in the form of short gravity waves on long waves and tidal currents *J. Fluid Mech.* **8**, 565–583.

Maniar, H. D. & Newman, J. N. 1996 Wave diffraction by a long array of circular cylinders In *Proc. 11th Int. Workshop on Water Waves and Floating Bodies, Hamburg, Germany, 17–20 March 1996* (ed. V. Bertram).

Mehlum, E. 1993 Splines and ocean wave modelling. Report STF A93008, SINTEF, Oslo, Norway.

Molin, B. 1979 Second-order diffraction loads on three-dimensional bodies. *Appl. Ocean Res.* **1**, 197–212.

Moubayed, W. I. & Williams, A. N. 1995 Second-order hydrodynamic interactions in an array of vertical cylinders in bichromatic waves. *J. Fluids Struct.* **9**, 61–98.

Newman, J. N. 1996 The second order wave force on a vertical cylinder. *J. Fluid Mech.* **320**, 417-443.

Price, W. G. & Bishop, R. E. D. 1974 *Probabilistic theory of ship dynamics*. London: Chapman and Hall.

Rainey, R. C. T. 1995 Slender-body expressions for the wave load on offshore structures. *Proc. R. Soc. Lond.* A **450**, 391–416.

Stokes, G. G. 1847 On the theory of oscillatory waves. *Trans. Camb. Phil. Soc.* **8**, 441–455.

Tromans, P. S., Anaturk, A. & Hagemeijer, P. 1991 A new model for the kinematics of large ocean waves—application as a design wave. In *Proc. 1st Int. Conf. Offshore and Polar Engineering, Edinburgh*, vol. 3, pp. 64–71.

Wu, G. X. 1991 On the second order wave reflection and transmission by a horizontal cylinder. *Appl. Ocean Res.* **13**, 58–62.

Wu, G. X. & Eatock Taylor, R. 1994 Finite element analysis of two-dimensional nonlinear transient water waves. *Appl. Ocean Res.* **16**, 363–372.

Wu, G. X. & Eatock Taylor, R. 1995 Time stepping solutions of the two-dimensional nonlinear wave radiation problem. *Ocean Engng* **22**, 785–798.

Wu, G. X., Ma, Q. W. & Eatock Taylor, R. 1996 Analysis of the interactions between nonlinear waves and bodies by domain decomposition. In *Proc. 21st Symp. on Naval Hydrodynamics, Trondheim, Norway, 24–28 June 1996*.

PHILOSOPHICAL TRANSACTIONS OF THE ROYAL SOCIETY A MATHEMATICAL, PHYSICAL & ENGINEERING SCIENCES